

# Primary energy reconstruction from the S(500) observable recorded with the KASCADE-Grande

G. Toma<sup>5</sup>, W.D. Apel<sup>1</sup>, J.C. Arteaga-Velázquez<sup>2</sup>, K. Bekk<sup>1</sup>, M. Bertaina<sup>3</sup>, J. Blümer<sup>1,4</sup>, H. Bozdog<sup>1</sup>, I.M. Brancus<sup>5</sup>, E. Cantoni<sup>3,6</sup>, A. Chiavassa<sup>3</sup>, F. Cossavella<sup>4</sup>, K. Daumiller<sup>1</sup>, V. de Souza<sup>7</sup>, F. Di Pierro<sup>3</sup>, P. Doll<sup>1</sup>, R. Engel<sup>1</sup>, D. Fuhrmann<sup>8</sup>, A. Gherghel-Lascu<sup>\*5</sup>, H.J. Gils<sup>1</sup>, R. Glasstetter<sup>8</sup>, C. Grupen<sup>9</sup>, A. Haungs<sup>1</sup>, D. Heck<sup>1</sup>, J.R. Hörandel<sup>10</sup>, D. Huber<sup>4</sup>, T. Huege<sup>1</sup>, K.-H. Kampert<sup>8</sup>, D. Kang<sup>4</sup>, H.O. Klages<sup>1</sup>, K. Link<sup>4</sup>, P. Łuczak<sup>11</sup>, H.J. Mathes<sup>1</sup>, H.J. Mayer<sup>1</sup>, J. Milke<sup>1</sup>, B. Mitrica<sup>5</sup>, C. Morello<sup>6</sup>, J. Oehlschläger<sup>1</sup>, S. Ostapchenko<sup>12</sup>, N. Palmieri<sup>4</sup>, T. Pierog<sup>1</sup>, H. Rebel<sup>1</sup>, M. Roth<sup>1</sup>, H. Schieler<sup>1</sup>, S. Schoo<sup>1</sup>, F.G. Schröder<sup>1</sup>, O. Sima<sup>13</sup>, G.C. Trinchero<sup>6</sup>, H. Ulrich<sup>1</sup>, A. Weindl<sup>1</sup>, J. Wochele<sup>1</sup>, J. Zabierowski<sup>11</sup> - KASCADE-Grande Collaboration

The primary energy is reconstructed in a standard approach at KASCADE-Grande based on a correlation between the total shower size and the muon size that are estimated on an event by event basis. In this paper we present a second approach to reconstruct the primary energy from the S(500) observable which is the charged particle density at a fixed radial range from the shower axis. CORSIKA simulations with QGSJet-II-2 model have shown that at this particular distance the charged particle density becomes independent of the primary mass and can be used as a primary energy estimator. A simulation-derived calibration is used to convert the recorded S(500) values into primary energy. The comparison between the result of the described method and the results of the standard approach reveals a systematic difference which cannot be explained entirely by the associated systematic uncertainties. We conclude that the source of this discrepancy is the inability of simulations to describe with sufficient accuracy the shape of the lateral distributions.

The 34th International Cosmic Ray Conference, 30 July- 6 August, 2015 The Hague, The Netherlands

<sup>&</sup>lt;sup>1</sup> Institut für Kernphysik, KIT - Karlsruhe Institute of Technology, Germany

<sup>&</sup>lt;sup>2</sup> Universidad Michoacana, Inst. Física y Matemáticas, Morelia, Mexico

<sup>&</sup>lt;sup>3</sup> Dipartimento di Fisica, Università degli Studi di Torino, Italy

<sup>&</sup>lt;sup>4</sup> Institut für Experimentelle Kernphysik, KIT - Karlsruhe Institute of Technology, Germany

<sup>&</sup>lt;sup>5</sup> Horia Hulubei National Institute of Physics and Nuclear Engineering, Bucharest, Romania

<sup>&</sup>lt;sup>6</sup> Osservatorio Astrofisico di Torino, INAF Torino, Italy

<sup>&</sup>lt;sup>7</sup> Universidade São Paulo, Instituto de Física de São Carlos, Brasil

<sup>&</sup>lt;sup>8</sup> Fachbereich Physik, Universität Wuppertal, Germany

<sup>&</sup>lt;sup>9</sup> Department of Physics, Siegen University, Germany

<sup>&</sup>lt;sup>10</sup> Dept. of Astrophysics, Radboud University Nijmegen, The Netherlands

<sup>&</sup>lt;sup>11</sup> National Centre for Nuclear Research, Department of Astrophysics, Lodz, Poland

<sup>&</sup>lt;sup>12</sup> Frankfurt Institute for Advanced Studies (FIAS), Frankfurt am Main, Germany

<sup>13</sup> Department of Physics, University of Bucharest, Bucharest, Romania E-mail: gabriel.toma@outlook.de

#### 1. Introduction

The primary energy is reconstructed in a standard approach at KASCADE-Grande [1] from a correlation between the total shower size and the muon size which are recorded on an event by event basis [2, 3, 4]. In this paper we present the result of a second approach in which the primary energy is inferred from the recorded charged particle density at 500 m from the shower axis, S(500). It has been shown [5] that for a given primary energy there exists a radial distance from the shower axis where the charged particle density becomes independent of the primary mass and can be used as a primary energy estimator. In the context of the KASCADE-Grande experiment, studies on simulated showers [6] (with CORSIKA [7] and the QGSJet-II-2 [8] hadronic interaction model) have shown this effect for a radial distance of about 500 m (Fig. 1). The S(500) is therefore characteristic to KASCADE-Grande and is also model-specific.

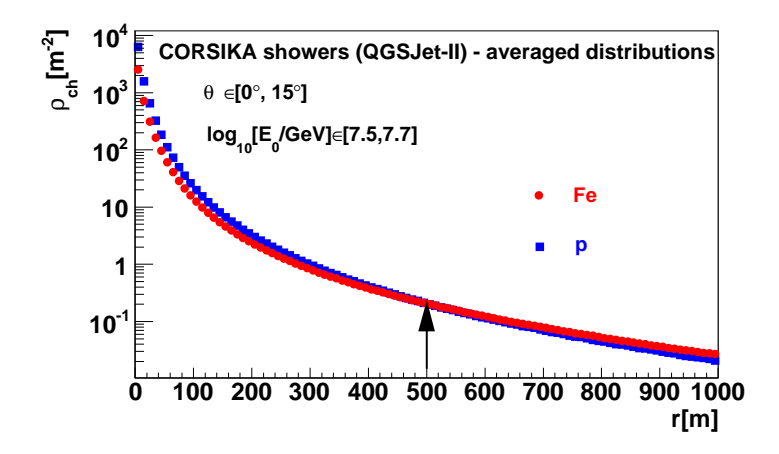


**Figure 1:** Averaged simulated lateral distributions for p and Fe primaries with energy in a narrow range.

## 2. KASCADE-Grande

KASCADE-Grande was hosted by the Karlsruhe Institute of Technology - KIT, Campus Nord, Germany (49°N, 8°E) at 110 m a.s.l. It had a roughly rectangular shape with a length of  $\approx$ 700 m. The KASCADE-Grande detector was an extension of the smaller detector array KASCADE [9]. The extension was guided by the intention to extend the energy range for efficient EAS detection to the energy interval of  $10^{16}$ - $10^{18}$  eV. The study described in this paper relies only on data recorded by the Grande component (Fig. 2), a detector array of 37 scintillator stations with an area of  $\approx$ 10 m<sup>2</sup> each.

#### 3. Shower selection

Two sets of showers are analyzed in both reconstruction approaches: one simulated with the CORSIKA tool (with the QGSJet-II-2 model embedded for high energy hadronic interactions)

<sup>\*</sup>Speaker.

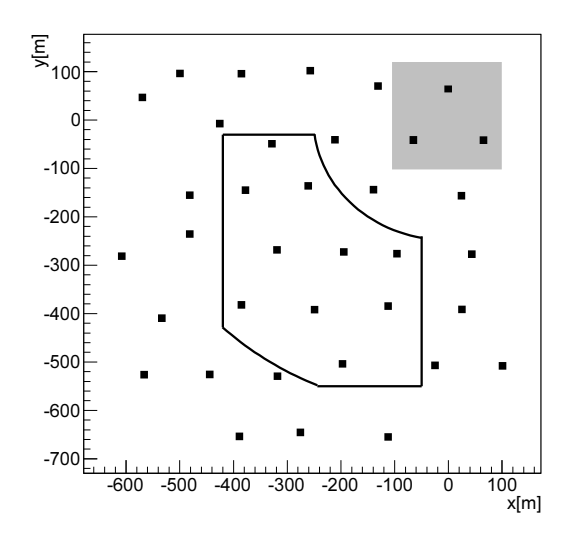


**Figure 2:** Schematic top-view of the KASCADE-Grande detector array (the Grande stations are shown as square dots; the fiducial area with line contour; the area covered by KASCADE as shaded rectangle).

and an experimentally recorded shower sample. The reconstruction procedure and the shower selection criteria are applied identically to simulated and experimentally recorded showers. The simulated shower sample includes events simulated for 5 primary (p, He, C, Si and Fe in fairly equal proportions) with continuous energy spectra between  $10^{15}$  -  $3 \times 10^{18}$  eV and with a spectral index  $\gamma$ =-2. A weighting is applied to simulated events in most of the subsequent studies to emulate a softer energy spectrum  $\gamma$ =-3 which is more similar to the one in the data. About  $3 \times 10^5$  events have been simulated for each primary. The arrival direction of showers is isotropical and the shower cores are spread randomly on an area larger than the Grande array. For experimental data the total acquisition time is 1503 days leading to an exposure of  $1.66 \times 10^{13}$  m<sup>2</sup>s sr. The main shower selection criteria dictate that the showers are inclined up to  $30^\circ$ , a minimum of 25 stations are triggered and a lateral particle density distribution is successfully parameterized with a 3-parameter Linsley function [10]. The fiducial area used for shower core selection (Fig. 2) was chosen as in the standard approach (to facilitate comparison between the two methods). Approximately  $9.05 \times 10^5$  experimental events have passed all imposed selection cuts.

## 4. The reconstruction procedure

To derive the primary energy, the S(500) observable is reconstructed first. The S(500) reconstruction starts from the energy deposits of secondaries in the detector stations. The energy deposits are converted into particle densities by employing lateral energy correction functions which take into account the angle of incidence of particles in detectors. The recorded charged particle densities are then projected in the plane normal to the shower axis. The charged particle distribution is then parameterized with a Linsley function and the charged particle density is inferred at 500 m from the shower axis. For primary energies above  $log_{10}[E_0/GeV]=7.5$  the fraction of showers with successfully reconstructed S(500) exceeds 95% (Fig. 3). On average, showers of identical primary

(mass and energy) will be attenuated differently in the atmosphere depending on their angle of incidence. To account for this effect, we correct the recorded S(500) values on an event by event basis using the Constant Intensity Cut method [12]. The primary energy is derived from the S(500) by employing a simulation-derived calibration (Fig. 4).

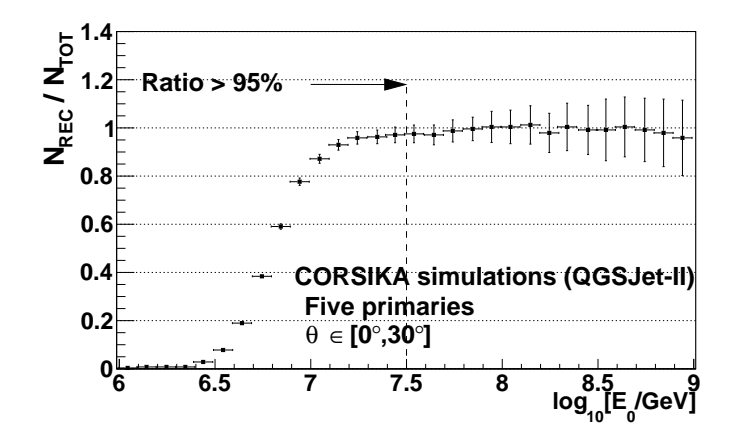


**Figure 3:** Ratio between the number of simulated events for which S(500) was successfully reconstructed and the total number of simulated events as a dependence with the primary energy.

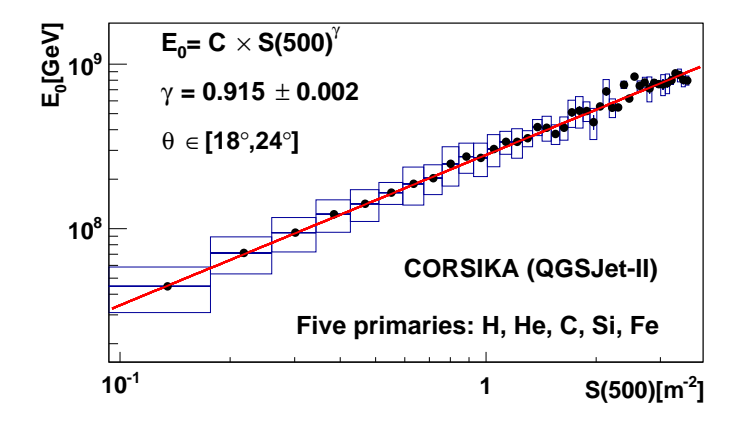


**Figure 4:**  $E_0$  - S(500) correlation; the dots are the profile of the scatter plot with box errors showing the spread of data while errors of the mean are dot sized; the continuous line is a power law fit.

#### 5. Comparison with the standard approach

We compare the reconstructed primary energy in the two approaches, for the same shower samples. Fig. 5 shows the reconstruction quality for simulated showers. In this case there is reasonable agreement between the two methods. In the case of experimental data the S(500)-derived primary energy is systematically higher when compared to the values from the standard approach (Fig. 6), a feature which diminishes towards higher energies. After evaluating the methods-specific systematics we conclude that this discrepancy cannot be entirely explained by systematics. As the reconstruction in both approaches is applied identically to simulated and recorded showers, we

anticipate that the source of this discrepancy might be the inability of simulations to describe all shower features with the same level of accuracy. When plotting simulated and experimental averaged charged particle lateral density distributions for fixed S(500) values, the data appears outside the p and Fe prediction of QGSJet-II-2 (Fig. 7). Towards large radial ranges and for a given shower size the simulated distributions are steeper than the measured one, which produces S(500) values smaller than those observed in data. Fig. 8 shows this effect.

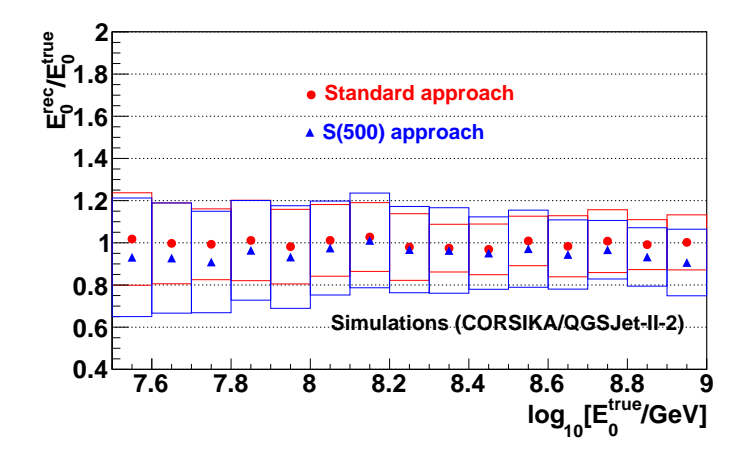


**Figure 5:** Comparison between methods when reconstructing simulated events: ratio between the reconstructed primary energy and the true energy as a function of the primary energy (the boxes show the spread of data).

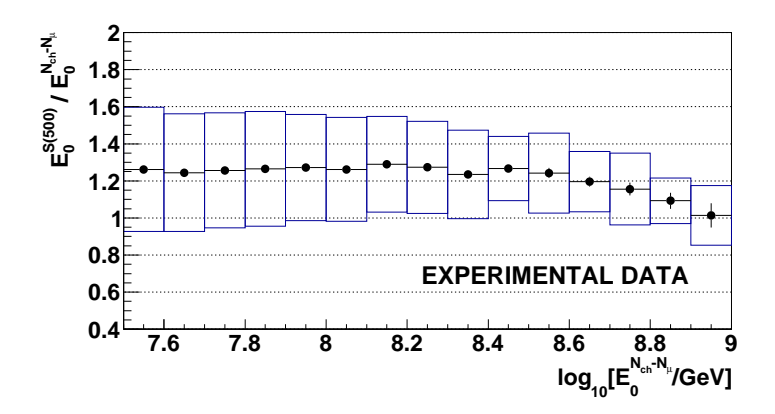


**Figure 6:** Comparison between methods when reconstructing experimental data: ratio between the S(500)-derived primary energy  $(E_0^{S(500)})$  and the reconstructed primary energy in the standard approach  $(E_0^{N_{ch}-N_{\mu}})$  (the boxes show the spread of data).

## 6. Conclusions

The primary energy has been reconstructed at KASCADE-Grande using the S(500) as primary energy estimator. The study has been applied on simulated and recorded showers and the results

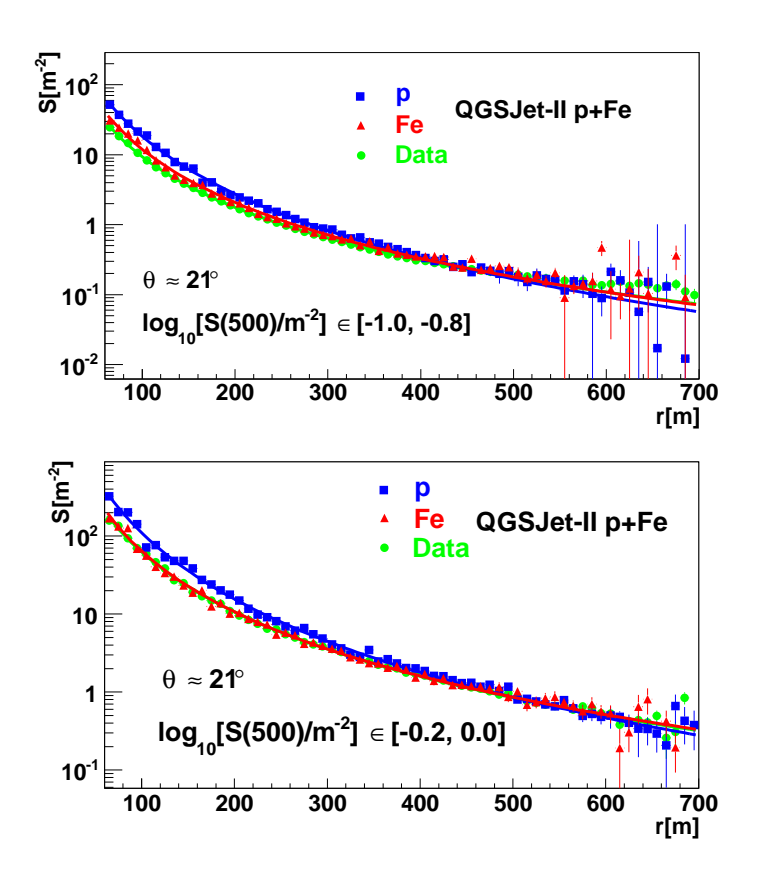


**Figure 7:** Averaged lateral charged particle density distributions for simulations (CORSIKA/QGSJet-II-2 p and Fe showers) and experimental data, for events with  $\log_{10}[S(500)/m^{-2}] \in [-1, -0.8]$  (above) and  $\log_{10}[S(500)/m^{-2}] \in [-0.2, 0.0]$  (below); we show only events inclined at  $\approx 21^{\circ}$  to avoid effects induced by attenuation in the atmosphere; the continuous lines are of a Linsley-type function.

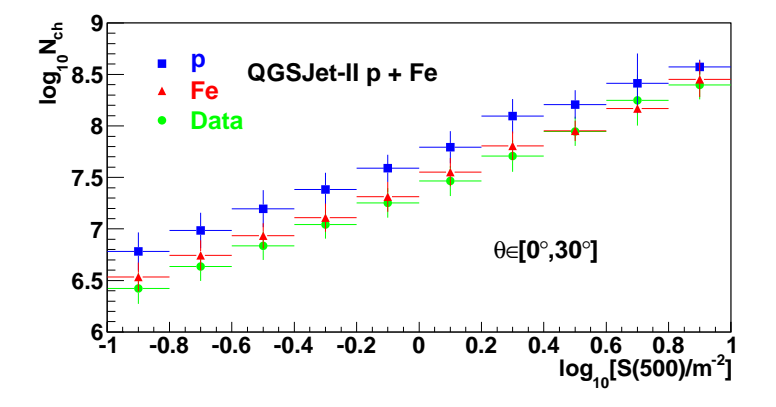


**Figure 8:** The correlation between the shower size  $N_{ch}$  (as derived in the standard approach) and the S(500) for p and Fe simulated events and for experimental data.

have been compared with the results of the standard reconstruction. The methods agree reasonably well when simulated events are analyzed. For experimental data the S(500)-derived primary energy appears systematically shifted towards higher energies when compared to the result of the

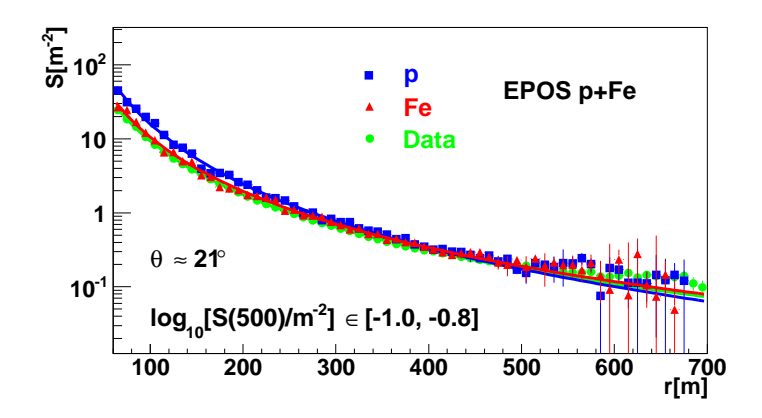


**Figure 9:** Averaged lateral charged particle density distributions for simulations (CORSIKA/EPOS 1.99 p and Fe showers) and experimental data, for events with  $\log_{10}[S(500)/m^{-2}] \in [-1, -0.8]$ .

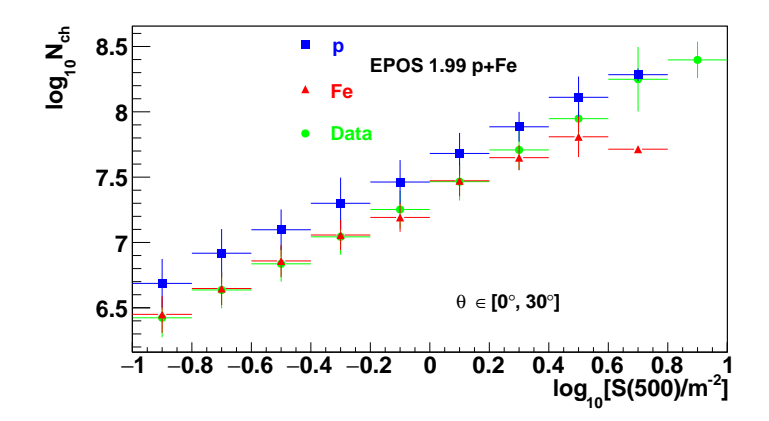


**Figure 10:** The correlation between the shower size  $N_{ch}$  (as derived in the standard approach) and the S(500) for p and Fe simulated events (with EPOS 1.99) and for experimental data.

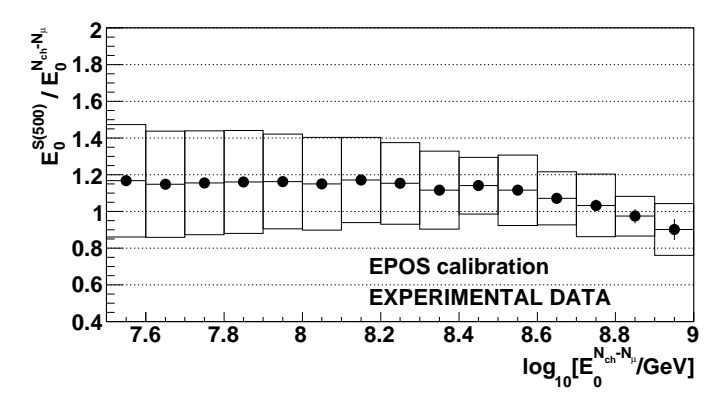


**Figure 11:** Ratio between the S(500)-derived primary energy  $(E_0^{S(500)})$  and the reconstructed primary energy in the standard approach  $(E_0^{N_{ch}-N_{\mu}})$  when the  $E_0^{S(500)}$  is inferred using a calibration based on simulations with EPOS 1.99.

standard reconstruction. This effect is mostly caused by the inability of simulations to accurately describe the shape of the charged particle lateral distribution. Reducing the data input to just one parameter (S(500)), and in the light of various approximations, we have to envisage limitations of the S(500) method. Compared to the standard approach (which extracts information from the entire radial range of lateral density distributions) the method based on the S(500) is more sensitive to fluctuations in the simulated shape of the lateral distribution. To improve the agreement between the simulated lateral distributions and the measured one a solution is to flatten the simulated lateral distributions at larger radial ranges. This can be achieved by increasing the overall muon content of showers or by adjusting the muon spatial distribution. A preliminary test with simulations based on EPOS 1.99 which introduces more muons than QGSJet-II-2, shows promising results (Fig. 9, 10, 11). Additional tests with more recent high energy hadronic interactions models (i.e. EPOS-LHC and QGSJet-II-4) are in progress.

## Acknowledgement

The authors would like to thank the members of the engineering and technical staff of the KASCADE-Grande collaboration, who contributed to the success of the experiment. The KASCADE-Grande experiment is supported in Germany by the BMBF and by the 'Helmholtz Alliance for Astroparticle Physics - HAP' funded by the Initiative and Networking Fund of the Helmholtz Association, by the MIUR and INAF of Italy, the Polish Ministry of Science and Higher Education, and the Romanian National Authority for Scientific Research, ANCS-UEFISCDI, project numbers PN-II-ID-PCE-2011-3-0691 and PN-II-RUPD-2011-3-0145. G. Toma acknowledges KIT Karlsruhe for supporting and hosting part of this research activity and also DAAD for supporting part of the study in the frame of the doctoral scholarship A/06/09016 Ref. 322.

#### References

- [1] W.D. Apel et al., The KASCADE-Grande experiment, NIM A 620 (2010) 202
- [2] W.D. Apel et al. (KASCADE-Grande collaboration), Astropart. Phys. 36 (2012) 183-194
- [3] W.D. Apel et al. (KASCADE-Grande Collaboration), Physical Review Letters 107 (2011) 171104
- [4] W.D. Apel et al. (KASCADE-Grande Collaboration), Physical Review D 87, 081101(R) (2013)
- [5] A.M. Hillas, J. Phys. G: Nucl. Part. Phys. 31 (2005) R95
- [6] H. Rebel and O. Sima et al. KASCADE-Grande collaboration, Proc. 29<sup>th</sup> ICRC Pune India 6 (2005) 297; I.M. Brancus et al. KASCADE-Grande collaboration, Proc. 29<sup>th</sup> ICRC Pune India 6 (2005) 361
- [7] D. Heck et al., Report Forschungszentrum Karlsruhe 6019 (1998)
- [8] N.N. Kalmykov, S.S. Ostapchenko and A.I. Pavlov, Nucl. Phys. B (Proc. Suppl.) 52B (1997) 17-28;
  S.S. Ostapchenko, Nucl. Phys. B-Proc. 151 (2006) 143-147;
  S.S. Ostapchenko, Phys. Rev. D 74 (2006) 014026
- [9] T. Antoni et al., The Cosmic-Ray Experiment KASCADE, NIM A 513 (2003) 490
- [10] J. Linsley et al., Journ. Phys. Soc. Japan 17 (1962) A-III
- [11] T. Antoni et al.: Astrop. Phys. 24 (2005) 1
- [12] M. Nagano et al., J.Phys G Nucl.Phys. 10 (1984) 1295